Biogeosciences Discuss., 11, 6419–6460, 2014
www.biogeosciences-discuss.net/11/6419/2014/
doi:10.5194/bgd-11-6419-2014

Biogeosciences Discussions
Open Access

Assessing the spatial variability in peak season CO_2 exchange characteristics across the Arctic tundra using a light response curve parameterization

H. N. Mbufong[1], M. Lund[1], M. Aurela[2], T. R. Christensen[1,3], W. Eugster[4], T. Friborg[5], B. U. Hansen[5], E. R. Humphreys[6], M. Jackowicz-Korczynski[3], L. Kutzbach[7], P. M. Lafleur[6], W. C. Oechel[8], F. J. W. Parmentier[1,3], D. P. Rasse[9], A. V. Rocha[10], T. Sachs[11], M. M. van der Molen[12], and M. P. Tamstorf[1]

[1]Arctic Research Center, Department of Bioscience, Aarhus University, Roskilde, Denmark
[2]Finnish Meteorological Institute, Helsinki, Finland
[3]Department of Physical Geography and Ecosystem Science, Lund University, Lund, Sweden
[4]ETH Zürich, Institute of Agricultural Sciences, Dept. Env. Systems Science, Zurich, Switzerland
[5]Department of Geography and Geology, University of Copenhagen, Copenhagen, Denmark
[6]Institute of Soil Science, University of Hamburg, Hamburg, Germany
[7]Department of Geography, Trent University, Trent, Canada
[8]Department of Biology, San Diego State University, San Diego, California, USA

[9]Bioforsk, Norwegian Institute for Agricultural and Environmental Research, Ås, Norway
[10]University of Notre Dame, Department of Biological Sciences, Notre Dame, USA
[11]Helmholtz Centre Potsdam, GFZ German Research Centre for Geosciences, Potsdam, Germany
[12]Meteorology and Air Quality group, Wageningen University, Wageningen, the Netherlands

Received: 3 March 2014 – Accepted: 10 April 2014 – Published: 6 May 2014

Correspondence to: H. N. Mbufong (henj@dmu.dk)

Published by Copernicus Publications on behalf of the European Geosciences Union.

BGD
11, 6419–6460, 2014

Abstract

This paper aims to assess the functional and spatial variability in the response of CO_2 exchange to irradiance across the Arctic tundra during peak season using light response curve (LRC) parameters. This investigation allows us to better understand the future response of Arctic tundra under climatic change. Data was collected using the micrometeorological eddy covariance technique from 12 circumpolar Arctic tundra sites, in the range of 64–74° N.

The LRCs were generated for 14 days with peak net ecosystem exchange (NEE) using an NEE -irradiance model. Parameters from LRCs represent site specific traits and characteristics describing: (a) NEE at light saturation (F_{csat}), (b) dark respiration (R_d), (c) light use efficiency (α), (d) NEE when light is at 1000 µmol m^{-2} s^{-1} (F_{c1000}), (e) potential photosynthesis at light saturation (P_{sat}) and (f) the light compensation point (LCP).

Parameterization of LRCs was successful in predicting CO_2 flux dynamics across the Arctic tundra. Yet we did not find any trends in LRC parameters across the whole Arctic tundra but there were indications for temperature and latitudinal differences within sub-regions like Russia and Greenland. Together, LAI and July temperature had a high explanatory power of the variance in assimilation parameters (F_{csat}, F_{c1000} and P_{sat}), thus illustrating the potential for upscaling CO_2 exchange for the whole Arctic tundra. Dark respiration was more variable and less correlated to environmental drivers than was assimilation parameters. Thus, indicating the inherent need to include other parameters such as nutrient availability, substrate quantity and quality in flux monitoring activities.

BGD
11, 6419–6460, 2014

1 Introduction

Arctic tundra ecosystems contain vast amounts of carbon (C) that could potentially be released to the atmosphere in a warming climate. It is, however, unclear how these carbon stocks are renewed by presently growing vegetation, and whether modern C sequestration rates vary among arctic tundra ecosystems and vegetation types. Using eddy covariance (EC) flux data from the few seasonally active long-term flux sites in the Arctic, we assessed ecosystem-scale growth and respiration rates using a light response approach to answer this question.

Arctic tundra ecosystems are unique ecosystems which have global implications for climate and global environmental change (Shaver et al., 1992). Although estimated to cover only 8 % of the global land surface (McGuire et al., 2009), they contain vast stocks of C stored in the permafrost, estimated to be in the order of 1400 to 1850 Pg C (Hugelius et al., 2013; Kuhry et al., 2009; McGuire et al., 2009; Schuur et al., 2008). Their climate and vegetation have been shown to be most sensitive to global change (ACIA, 2005; Oechel et al., 2000; SWIPA, 2011). A decade ago, studies still did not agree on whether this region is a net sink or source of carbon dioxide (CO_2) as individual site studies either proved insufficient or inconclusive in explaining this (Vourlitis and Oechel, 1997, 1999). Yet, recent estimates suggest that the Arctic tundra is most likely a net sink of CO_2 (IPCC, 2013), though whether it is a strong or weak sink needs to be further assessed (McGuire et al., 2012).

Previously, the Arctic tundra C budget has been estimated by using data from a few detailed study sites to extrapolate to the larger surrounding area (Williams et al., 2006), and by the application of regional process based models (McGuire et al., 2012). Scaling up from a few measurement sites to the circum-arctic region raises the question of representativeness of sites and measurements. This also holds for the widely used EC methodology (Baldocchi, 2003) with which a footprint of typically a few tens of square-meters to a hectare of tundra surface is covered, from which conclusions should be drawn for a vast area where no measurements exist, but which shows a great

BGD
11, 6419–6460, 2014

between-ecosystem variability of flux rates that feedback with the regional climate system (Chapin et al., 2000). Hence, the derivation of functional relationships of assimilation and ecosystem respiration rates as a function of environmental drivers bears more potential for providing insights into the overall functioning of Arctic tundra vegetation as the interface between the vast below-ground C storages and the atmosphere. Simple models using leaf area (LAI), temperature and photosynthetically photon flux density (Shaver et al., 2013, 2007) have been shown to make reliable predictions of measured net ecosystem exchange (NEE) and its components at the plot scale ($\leq 1\,m^2$) in the Arctic tundra. Model parameters can then be examined for differences among sites related to differences in climatic and environmental conditions (Laurila et al., 2001; Williams et al., 2006).

Most Arctic tundra sites are characterized by small emissions of CO_2 during winter (Fahnestock et al., 1999; Jones et al., 1999) and by high uptake during the short growing season, which is often less than 100 days. Despite being short, the growing season has been shown to be most relevant in defining the spatial (Aurela et al., 2004; Kwon et al., 2006; Lund et al., 2010), and temporal variability (Griffis et al., 2000; Groendahl et al., 2007; Lund et al., 2012) in net ecosystem C budgets of Arctic tundra. During this period, there is a net uptake of CO_2 from the atmosphere, which is characterized by a seasonal trend, peaking shortly after midsummer, i.e. July (Groendahl et al., 2007). In the Arctic tundra, peak season coincides with maximum air temperature leading to the highest plants growth rates. Consequently, plant reach their maximum leaf area towards the end of that period. It should be noted that light is not a limiting factor (Oberbauer et al., 1998) as the sun does not set during peak season. However, this complicates the accurate determination of ecosystem respiration with the EC approach (Eugster et al., 2005) under the absence of dark nights. The light response approach circumvents this problem (Gilmanov et al., 2003) by only using daytime data. Therefore, the light response method used with peak-season EC flux measurements from available long-term sites in the Arctic, seems the best approach to increase our understanding of how net CO_2 exchange and its gross components of assimilation

BGD
11, 6419–6460, 2014

and ecosystem respiration differ among tundra ecosystems. This study is the first to compare peak season NEE – irradiance characteristics at the landscape scale across different tundra types covering the entire circumpolar Arctic. We hypothesized that: (1) LRC parameters can be used to predict net ecosystem exchange dynamics across the Arctic tundra; (2) vegetation properties (e.g. LAI and NDVI), temperature and peak season phenology (start date) are the main drivers of Arctic tundra's NEE dynamics and (3) variability in Arctic tundra LRC characteristics follows a temperature and latitudinal gradient.

2 Materials and methods

2.1 Sites description

This study focuses on some of the most common types of tundra ecosystems across the circumpolar Arctic ranging from 64–74° N; including three Alaskan sites (US-Anak-LA, US-Barr-LA, US-Ivot-LA), one Canadian site (CA-Dar-LA), two Greenlandic sites (GL-Nuuk-LA, GL-Zack-HA), three Scandinavian sites (NO-Ando-SA, FI-Kaam-SA, SE-Stord-SA) and three Russian sites, i.e. RU-Kyt-LA, RU-Sam-LA and RU-Seid-SA (Fig. 1, Table 1). The sites range from peat bogs and fens to wet and dry tundra ecosystems; with and without permafrost. Site names used in the study are composed of country abbreviations (e.g. SE for Sweden and GL for Greenland), abbreviated site names (e.g. Stord for Stordalen and Zack for Zackenberg), and abbreviated Arctic tundra type (e.g. SA for Subarctic, LA for Low Arctic and HA for High Arctic). A detailed site description can be found in Table 1. Figure 1 illustrates site locations and Arctic flouristic boundaries (AMAP, 1998).

2.2 Data sets

The analyses in this study are based on eddy covariance (EC) measurements of net ecosystem exchange (NEE) of CO_2 alongside environmental variables. Environmental

BGD
11, 6419–6460, 2014

variables include photosynthetic photon flux density (PPFD), temperature (air and soil), soil moisture, precipitation and radiation (net and global). The length and range of measurements vary among sites from year round measurements to summer campaigns at the most inaccessible sites.

Various instruments for EC measurements have been used across the sites in this study, including analyzers such as the open-path LI-7500 (LiCor Inc., USA), closed-path LI-6262 and LI-7000 (LiCor Inc., USA), and the open-path IRGA designed by NOAA's Atmospheric Turbulence and Diffusion Division (ATDD). In this study, we have only examined peak season data, a period during which snow and moisture obstructions of the infrared path, as well as the surface self-heating issue (Burba et al., 2008) on open path systems are expected to be either minimal or inexistent. Wind velocity and temperature has been measured using 3-D sonic anemometers (R2 and R3, Gill Instruments, UK; CSAT3, Campbell Sci., UK; and SWS-211, Applied Technologies). The frequency of CO_2 flux signal measurements ranged from 5 to 20 Hz depending on the site. Varying data collection frequency between 5 and 10 Hz did not significantly affect resulting fluxes in Kytalyk (van der Molen et al., 2007). With the exception of Samoylov Island, with one hourly averaged flux data, all sites have averaged flux data into 30 min averages. Quantum sensors (Models Li-190SA, Li-190SB and Li-190SZ, LiCor Inc., USA) have been used to measure photosynthetic photon flux density (PPFD, $\mu mol\, m^{-2}\, s^{-1}$). For Kytalyk, where there were no direct PPFD measurements, estimates were made from global incoming radiation assuming a linear relationship (Jacovides et al., 2003). Table 1 summarizes ecosystem characteristics and EC instrumentation and setup across sites in this study.

The raw data from the EC systems has been processed using standard procedures (Aubinet et al., 2000; Baldocchi et al., 2001). It is imperative that standardized post processing procedures are used so as to avoid bias introduced by different flux correction approaches (Lund et al., 2010). Details of the EC post processing corrections are found in the relevant publications for each site: US-Anak-LA (Rocha and Shaver, 2011), US-Barr-LA and US-Ivot-LA (Kwon et al., 2006), CA-Dar-LA (Lafleur and Humphreys,

BGD
11, 6419–6460, 2014

2008), FI-Kaam-SA (Aurela et al., 2001), RU-Kyt-LA (Parmentier et al., 2011), NO-Ando-SA, GL-Nuuk-LA and GL-Zack-HA (Lund et al., 2012), RU-Sam-LA (Kutzbach et al., 2007; Runkle et al., 2013), RU-Seid-SA (Marushchak et al., 2013), and SE-Stord-SA (Christensen et al., 2012).

2.3 Data analyses

Growing season was calculated as the period from the first to the last day of net daily uptake of CO_2. We split each growing season into 14 days segments and carried out light response curve (LRC) analyses on these segments, using the *Misterlich* function (Falge et al., 2001):

$$\mathrm{NEE} = -(F_{\mathrm{csat}} + R_{\mathrm{d}})\left(1 - e^{\frac{-\alpha(\mathrm{PPFD})}{F_{\mathrm{csat}}+R_{\mathrm{d}}}}\right) + R_{\mathrm{d}}. \quad (1)$$

This function has three parameters (F_{csat}, α, R_{d}) that were obtained via least-squares fitting in Matlab R2010 (The Mathworks Inc., USA) to observed daytime (PPFD > 10 µmol m^{-2} s^{-1}) values of NEE (µmol m^{-2} s^{-1}), using PPFD (µmol m^{-2} s^{-1}) as the single environmental driving variable. The flux at light saturation (F_{csat}) parameter is the maximum net CO_2 uptake – i.e. when further increases in PPFD do not affect the uptake of CO_2 by the vegetation (in µmol m^{-2} s^{-1}). The parameter R_{d} illustrates dark respiration, i.e. the CO_2 flux when PPFD equals 0 (also given in µmol m^{-2} s^{-1}). Light use efficiency, also known as quantum yield (α), is the initial rate of change in NEE with increasing PPFD. Other functional parameters examined include the flux when PPFD equals 1000 in µmol m^{-2} s^{-1} (F_{c1000}); potential photosynthesis at light saturation (P_{sat}), calculated as $F_{\mathrm{csat}} + R_{\mathrm{d}}$; and the light compensation point (LCP), illustrating the light level at which the ecosystem switched from a net source to a net sink (PPFD when NEE = 0 µmol m^{-2} s^{-1}). Figure B1a–e illustrates the parameterization of LRC using Eq. (1). The 14 days period with maximum F_{csat} is hereafter referred to as the peak season. This period is characterized by maximum light levels as the sun never sets be-

BGD
11, 6419–6460, 2014

low the horizon. Also, vegetation is at its peak (maximum NDVI and LAI) with highest plant growth rates coinciding with maximum air temperatures.

These parameters were then compared among sites to identify the variability of the Arctic tundra. This approach is advantageous for inter-site comparisons because sites can readily be compared irrespective of varying meteorological conditions (Laurila et al., 2001). The *Misterlich* function (Falge et al., 2001) is ideal for such a comparison as it assumes a more realistic upper limit for NEE, with a clearly defined value at high PPFD and a stronger curvature than the rectangular hyperbola (Fig. B2).

For comparison with other studies, we have used results from previous studies that compared Greenland, Finland, and Norway (Laurila et al., 2001); and Greenland and Sweden (Frolking et al., 1998). These studies have used a rectangular hyperbolic function:

$$\mathrm{NEE} = \frac{\alpha_2 \cdot \mathrm{PPFD} \cdot P_{\max}}{\alpha_2 \cdot \mathrm{PPFD} + P_{\max}} + R. \quad (2)$$

The resulting parameter $P_{\max}$ refers to potential photosynthesis at light saturation, R is dark respiration while α_2 is the initial slope of the light response curve or light use efficiency. The parameters R_d and α from Eq. (1) are comparable to R and α_2 from Eq. (2), respectively (Fig. B2), whereas $P_{\max}$ from Eq. (2) is consistently showing more negative values than P_{sat} (Fig. B3), due to an unrealistic increase in NEE (in absolute terms) at high light levels in Eq. (2) (Fig. B2).

For sites with multi-year data, LRC parameters and ancillary variables were averaged for corresponding peak periods and error bars indicate standard deviations among site years. In order to investigate the drivers of variability in peak season LRC parameters across the Arctic, regression analyses with phenological variables – such as growing season start, growing season length and peak season start – were performed using the linear regression tool in IBM SPSS Statistics 20. Furthermore, mean environmental variables for July – e.g. air and soil temperature, soil moisture, vapor pressure deficit (VPD), relative humidity, incoming and outgoing shortwave radiation, net radia-

BGD
11, 6419–6460, 2014

tion, precipitation and PPFD, were also used. Maximum leaf area index (LAI) was extracted from referenced literature (Lafleur et al., 2012; Laurila et al., 2001; Lund et al., 2010; Marushchak et al., 2013), while normalized difference vegetation index (NDVI) data was retrieved from MODIS Land Product Subsets (http://daac.ornl.gov/MODIS/) as 250 m × 250 m pixel in the dominant wind direction and within the footprint of the flux tower. The coefficient of variation (CV), calculated by dividing the standard deviation by the mean, has been used to compare the variation among LRC parameters across the Arctic. Curve estimation and regression analysis were done using an analyses of variance (ANOVA) for linear relationships using the curve estimation tool (IBM SPSS Statistics 20). Multiple linear regressions (step-wise) were used to investigate the combined control of environmental variables on LRC parameters using the linear regression tool (IBM SPSS Statistics 20).

3 Results and discussion

A multiple linear regression using maximum LAI and July air temperature as independent variables was found to strongly explain plant growth across 12 Arctic tundra sites as expressed by the assimilation parameters (P_{sat}, F_{c1000} and F_{csat}) of the LRC (Table 2). A maximum of 93 % of the variability in F_{c1000} could be explained, and similar performance of the model was found for F_{csat} (92 %) and P_{sat} (90 %). Shaver et al. (2013) developed a model for predicting NEE based on short-term small scale chamber flux measurements ($\leq 1\,m^2$) from various ecosystems types within five Arctic sites (including US-Barr-LA, SE-Stord-SA and GL-Zack-HA in this study) using LAI (estimated from NDVI), air temperature and PPFD. Their model explained ca. 75 % of the variation in NEE across Arctic ecosystems. The main advantage of using landscape scale eddy covariance (EC) data compared with plot scale chamber data is that EC data integrates fluxes over a larger area, which thus makes it more readily comparable with satellite-derived information. Despite differences in scale and model parameteri-

BGD
11, 6419–6460, 2014

zations, our results confirm the findings of Shaver et al. (2013) on the great potential in using LAI, NDVI, air temperature and irradiance for upscaling Arctic CO_2 exchange.

Maximum LAI alone explained 70 to 75 % (Fig. 2, Table 2) of the assimilation parameters suggesting that direct measurements of leaf area could be useful in estimating photosynthesis from tundra ecosystems. Remotely sensed NDVI was not quite as powerful in explaining plant growth; NDVI explained 59 to 67 % of the variance in assimilation parameters (Fig. 3, Table 2). Generally, LAI exerted stronger controls on LRC parameters than NDVI (Figs. 2 and 3). Using LAI is advantageous as it is a real and physical vegetation property, directly measured through plot sampling and shown to be directly linked to C exchange while NDVI is a surrogate vegetation property often used to estimate LAI (Shaver et al., 2013, 2007). In our study, LAI data was available for only nine sites as opposed to twelve for NDVI. Given the differences in measurement methodology and instrumentations, comparing LAI among sites may introduce uncertainty in the estimates. LAI used herein is for vascular plant cover only (Ross, 1981), thereby ignoring non-vascular plants like mosses, which are known to contribute significantly to Arctic ecosystem CO_2 exchange (Street et al., 2012). Satellite derived indices like NDVI may also be useful as similar calculation methods have been used and there is a possibility of upscaling for the whole Arctic tundra as satellite derived NDVI data are readily available (Loranty et al., 2011). Despite the shortcomings of LAI and NDVI, they have been shown to satisfactorily estimate gross primary productivity (GPP) (r^2 = 0.78 – 0.81) in northern Scandinavia and Alaska (Street et al., 2007). In general, all LRC parameters had a significant, or, in the case of α, close to significant (p = 0.09) relationship with NDVI, illustrating the potential to use Earth observation products for spatial integration.

On its own, temperature was the least significant driver of variations in LRC parameters, explaining only about 32 % to 35 % of F_{csat}, P_{sat} and F_{c1000} respectively (Table 2). Yet, in combination with LAI, control on assimilation parameters was greatly improved (Table 2) as warming increases the productive capacity and leaf area of most plant species (Walker et al., 2003). This could be explained by the fact that higher temper-

BGD
11, 6419–6460, 2014

atures increase weathering, nitrogen fixation (Sorensen et al., 2006) and soil organic matter decomposition (Robinson et al., 1997) thereby increasing soil nutrient availability. There is, therefore, an urgent need for standardized routines for monitoring other aspects that are not covered at several sites across the Arctic tundra like nutrient availability and substrate quality.

It was interesting to notice that mean July air temperature seemed to exert stronger controls on F_{csat}, P_{sat} and F_{c1000} (assimilation parameters) than on R_d. A steeper slope ($0.3-0.4\,\mu mol\,CO_2\,m^{-2}\,s^{-1}\,K^{-1}$) of the temperature vs. assimilation parameters regressions (Table 2) as opposed to temperature vs. R_d ($0.1\,\mu mol\,CO_2\,m^{-2}\,s^{-1}\,K^{-1}$) suggested that an increase in temperature would cause an increase in net CO_2 uptake during peak season for the ecosystems in this study, thereby strengthening the sink function of the Arctic tundra, if no other factors are considered. One limitation of modeling photosynthesis and respiration as a function of environmental variables is that these physiological properties tend to undergo different degrees of acclimation to some environmental variables. Ecosystems acclimate to warmer temperature by increasing the thermal optimum for their continued survival (Niu et al., 2012). Previous studies have shown a strong and independent thermal acclimation of photosynthesis (Baldocchi, 2008; Baldocchi et al., 2001; Mooney et al., 1978; Niu et al., 2008), ecosystem respiration (Baldocchi, 2008; Centritto et al., 2011; Ow et al., 2008a, b) and NEE (Yuan et al., 2011) at the level of the ecosystem. Short term monitoring in the High Arctic has suggested that photosynthesis and ecosystem respiration (Lund et al., 2012; Oechel et al., 2000) have increased with observed changes in climate, while NEE trends remain unclear (Lund et al., 2012).

We have identified that there is a large circumpolar variability in the light response and LRC parameters within the Arctic tundra. This is reflected in the varying shapes of LRC among the sites (Fig. 4a–c), thus, suggesting that Arctic tundra ecosystems are diverse and should not be treated as a single entity. We originally had expected that respiration rates from the generally waterlogged active layers typical of tundra ecosystems should respond more clearly and positively to temperatures. But the dark respira-

BGD
11, 6419–6460, 2014

tion (R_d) did not show a consistent temperature pattern, though it varied substantially among tundra sites (Tables 2 and 3). The correlations between R_d and vegetation indices (LAI and NDVI) were significant (Figs. 2b–3b; Table 2); however the relationships were weaker compared to those observed for assimilation parameters (Figs. 2–3a, d and e; Table 2). Previous research has shown that Arctic plants vary in their light responses and rates of photosynthesis (Bigger and Oechel, 1982; Chapin and Shaver, 1996; Oberbauer and Oechel, 1989). Similarly, a high inter-site variability of summertime NEE has been documented in another comparison study (Lund et al., 2010) on northern wetlands in northern Europe and North America. This is contrary to quantified variability in seven Canadian sites (Humphreys et al., 2006), where the rates of peak season NEE were comparable.

Though all sites attained peak productivity in July (Table 3), a regression analysis showed that the variability was unrelated to the start of the peak season and did not reveal any latitudinal dependency. Interestingly, the largest differences among LRC curves within the Low Arctic were seen between RU-Sam-LA and RU-Kyt-LA (Fig. 4b; Table 1). This may mean that geographical proximity and similar latitude are not the key factors that explain tundra ecosystem CO_2 fluxes. An examination of the coefficient of variation (CV) showed that the assimilation parameters (F_{csat}, F_{c1000} and P_{sat}) were less variable than R_d (Table 3) among study sites. This suggested that ecosystem respiration is the main driver of CO_2 flux variability in the Arctic tundra during peak season. Yet, comparable variability in photosynthesis and ecosystem respiration was found in seven Canadian Boreal peatlands (Humphreys et al., 2006) during peak season while in northern wetlands (Lund et al., 2010) and Canadian tundra (Lafleur et al., 2012) ecosystems, variability in NEE was driven mainly by photosynthesis. This may be because our study is circumpolar and comprises of a wide range of climate and ecosystem settings as opposed to northern wetlands (Lund et al., 2010) and the Canadian Boreal peatlands (Humphreys et al., 2006) and the Canadian tundra (Lafleur et al., 2012).

BGD
11, 6419–6460, 2014

The LCP is the light level at which the amount of CO_2 released through ecosystem respiration equals the amount taken up by plants during photosynthesis. This varies in response to a different vegetation composition and light conditions (Givnish, 1988; Givnish et al., 2004). The average light levels during peak season could explain about 50 % of LCP (Fig. 6, Table 2). In this study, LCP varied between 50 $\mu mol\,m^{-2}\,s^{-1}$ and 156 $\mu mol\,m^{-2}\,s^{-1}$, well above the estimated (33 $\mu mol\,m^{-2}\,s^{-1}$) rate for a temperate peatland (Shurpali et al., 1995) but within the estimated rates for *Sphagnum* dominated tundra ecosystems in the Low Arctic, 10–140 $\mu mol\,m^{-2}\,s^{-1}$ (Skre and Oechel, 1981). Previous studies have shown LCP to be lower for shade-grown than for sun-grown vegetation even when there is no significant difference in their photosynthetic parameters (Björkman et al., 1972; Givnish, 1988). This suggests that LCP may have no control on the C gain/loss of the ecosystem. Givnish (1988) therefore proposed that, for the compensation point to be meaningful, other vegetation costs related to night time leaf respiration, construction of plant stems, leaves and roots must be considered (effective compensation point).

Variability in local weather conditions has been shown to be largely responsible for between-year fluctuations in CO_2 flux components of northern ecosystems (Groendahl et al., 2007; Lafleur and Humphreys, 2008; Lund et al., 2012, 2010). In this study, for example, RU-Seid-SA consistently had the highest rates of LRC parameters (Fig. 5; Table 3); however, this was based on one single year of data (2008). Though 3–5 °C warmer than the long term July mean, 2008 July temperatures were lower than 2007 (Marushchak et al., 2013). Thus, we have further examined peak season for sites with available 2008 data (RU-Seid-SA, SE-Stord-SA, NO-Ando-SA, US-Anak-LA, RU-Kyt-LA, GL-Nuuk-LA, and GL-Zack-HA) to investigate whether the outlier was the year (2008) or the site (RU-Seid-SA). Mean July temperature was higher than average in RU-Seid-SA, US-Anak-LA and SE-Stord-SA but RU-Seid-SA was most extreme as its July temperature was > 1 stdev above the mean (Table A1). This was further emphasized as RU-Seid-SA was consistently higher (> 1 stdev) above the mean for 2008 in terms of LRC parameters. The high F_{csat} and α during the peak season in RU-Seid-SA

BGD
11, 6419–6460, 2014

illustrates the high photosynthetic capacity of this site but perhaps more interesting was the high R_d for this site, which considerably diminishes its sink function and reiterates the importance of soil characteristics.

Previous studies have used hyperbolic relationships between NEE and PPFD to estimate comparable parameters among sites (Frolking et al., 1998; Laurila et al., 2001; Ruimy et al., 1995). Though they used another function (Eq. 2), R and α_2 have been shown to be comparable with R_d and α from Eq. (1) in this study (Fig. B2). The apparent quantum yield parameter (α_2, the initial slope of the LRC) in Frolking et al. (1998) averaged at about 0.04 for peatlands (ca. 0.044 for fens; and ca. 0.031 for bogs). The fen values (Laurila et al., 2001) are comparable to estimates from wet sites in our study while the estimates for bogs (Frolking et al., 1998) are higher than observed in NO-Ando-SA (Table 3). This could be because NO-Ando-SA is more northerly situated and thus colder compared with sites in Frolking et al. (1998). Dark respiration was estimated to be between 4.0 to 6.6 $\mu mol\,m^{-2}\,s^{-1}$ for fens and 2.2 $\mu mol\,m^{-2}\,s^{-1}$ (Frolking et al., 1998) at a Swedish bog. These are higher than estimated in our study because our sites were located at higher latitudes (64–74° N) compared to 43° N to 56° N (Frolking et al., 1998). Dark respiration estimates from the only High Arctic site in our study (GL-Zack-HA) was similar to estimates from the same site based on earlier data from 1997 (Laurila et al., 2001) and at a nearby willow snow-bed (0.9 $\mu mol\,m^{-2}\,s^{-1}$), while a higher value was obtained from a nearby fen (2.3 $\mu mol\,m^{-2}\,s^{-1}$); all three sites being located within ca. 1 km from each other (Laurila et al., 2001), again demonstrating the heterogeneity of Arctic landscapes.

The possibility of explaining and modeling the variation of CO_2 exchange components based on controlling environmental drivers is essential to improve our understanding of current CO_2 exchange, and to correctly simulate the response of Arctic tundra to an expected change in climate (Lund et al., 2010). In follow-up studies, it is intended to model and upscale LRC parameters using the functional relationships with LAI, NDVI and air temperature across the Arctic tundra. Arctic vegetation data (e.g. LAI and NDVI) will be retrieved through remote sensing data e.g. the MODIS Land

BGD
11, 6419–6460, 2014

Product Subsets and circumpolar Arctic vegetation maps, CAVM (Walker et al., 2005) while climate data can be retrieved from global grid datasets such as Climatic Research Unit, CRU (New et al., 2002). Detangling the effects of a changing climate and reducing the level of uncertainties in the Arctic C balance estimations remains a highly prioritized topic for climate research. Combining increased monitoring activities and process-based studies using remote sensing tools and mechanistic modeling serves as the most plausible way forward to improve our understanding of the Arctic and global C cycle.

4 Conclusions

We have shown that LRC parameterization could be used successfully to predict NEE dynamics in the Arctic tundra. Though peak season phenology could not explain CO_2 exchange dynamics, a combination of vegetation properties (LAI) and temperature showed a strong positive relationship with assimilation parameters. Individual environmental variables were not as good in explaining variability in LRC parameters, especially respiration parameters, suggesting that these physiological parameters may acclimate to warmer temperatures. Also, some factors that are typically not included in eddy covariance CO_2 exchange studies (such as nutrient availability and substrate quantity and quality of soil organic matter) could be instrumental in explaining the spatial variability in CO_2 fluxes among Arctic tundra ecosystems. Across the whole Arctic tundra, this study did not find any temperature or latitudinal trends in LRC parameters. Latitudinal differences within sub-regions in Greenland and Russia were observed, however, these differences were more related to ecosystem type and characteristics than climatic settings.

Acknowledgements. We would like to thank the two anonymous reviewers for their valuable comments which were instrumental in improving this manuscript. We also thank NordForsk for funding the DEFROST project through its Top-Level Research Initiative (TFI), Nordic Center of Excellence (NCoE), through which this work is partly funded, and Aarhus University's Graduate

BGD
11, 6419–6460, 2014

School of Science and Technology for the rest of the funding. We are grateful to all the research teams and their funding sources. US-Anak-SA was funded by the National Science Foundation (NSF grant number 1065587); NO-Ando-SA was sponsored by Bioforsk, NILU – Norwegian Institute for Air Research and the Smithsonian Environmental Research Center, with funding from the Research Council of Norway (project NFR208424, GHG-NOR) and the Stiftelsen Fondet for Jord- og Myrundersøkelser; US-Barr-LA and US-Ivot-LA was funded by NSF (OPP-0421588 BE/CBC), NSF (ARC-1204263), Department of Energy, DOE (Terrestrial Carbon Cycle Research DE-SC0005160), the Carbon in Arctic Reservoirs Vulnerability Experiment (CARVE), an Earth Ventures (EV-1) investigation, under contract with the National Aeronautics and Space Administration (NASA); CA-Dar-LA was sponsored by the Natural Science and Engineering Research Council of Canada (NSERC); FI-Kaam-SA was funded by the European Commission (ENV4-CT95-0093) and the Academy of Finland; RU-Kyt-LA was supported by the Research council for Earth and Life Sciences (ALW) with financial aid from the Netherlands Organization for Scientific Research (NWO, grant no. 854.00.018), the Darwin Center for Biogeology of ALW/NWO, the European Commission under the Fifth Framework Programme TCOS-Siberia (EVK2-2001-00143), the NWO Dutch Russian research cooperation programme entitled "Long term observation of soil carbon and methane fluxes in Siberian tundra" (047.017.037), the GreenCyclesII training network (7th Framework programme reference 238366) and Darwin Center for Biogeosciences who supported with a grant to F. J. W. Parmentier (142.16.1041); monitoring in GL-Nuuk-SA and GL-Zack-HA was through the the GeoBasis and ClimateBasis programs of the Nuuk and Zackenberg Ecological Research Operations (NERO and ZERO) networks funded by the Danish Energy Agency; RU-Sam-LA and Torsten Sachs was supported through the Helmholtz Association (Helmholtz Young Investigators Group, grant VH-NG-821); RU-Seid-SA was funded by the EU 6th Framework Programme project CARBO-North (contract number 036993; www.carbonorth.net) and SE-Stord-SA was supported by the EU funded GREENCYCLES-RTN, Swedish Research Councils VR and FORMAS, the Danish Natural Science Research Council as well as the Crafoord foundation and the Royal Swedish Physiographical Society. We are also very grateful to all who have assisted in the collection of data for these study sites.

BGD
11, 6419–6460, 2014

References

ACIA: Arctic Climate Impact Assessment-Scientific Report, 1st edn., New York, 2005.

AMAP: AMAP Assessment Report: Arctic Pollution Issues, Arctic Monitoring and Assessment Programme (AMAP), Oslo, Norway, 859 pp., 1998.

Aubinet, M., Grelle, A., Ibrom, A., Rannik, U., Moncrieff, J., Foken, T., Kowalski, A. S., Martin, P. H., Berbigier, P., Bernhofer, C., Clement, R., Elbers, J., Granier, A., Grunwald, T., Morgenstern, K., Pilegaard, K., Rebmann, C., Snijders, W., Valentini, R., and Vesala, T.: Estimates of the annual net carbon and water exchange of forests: the EUROFLUX methodology, Adv. Ecol. Res., 30, 113–175, 2000.

Aurela, M., Laurila, T., and Tuovinen, J. P.: Seasonal CO_2 balances of a subarctic mire, J. Geophys. Res.-Atmos., 106, 1623–1637, 2001.

Aurela, M., Laurila, T., and Tuovinen, J. P.: The timing of snow melt controls the annual CO_2 balance in a subarctic fen, Geophys. Res. Lett., 31, L16119, doi:10.1029/2004GL020315, 2004.

Baldocchi, D.: Breathing of the terrestrial biosphere: lessons learned from a global network of carbon dioxide flux measurement systems, Aust. J. Bot., 56, 1–26, 2008.

Baldocchi, D. D.: Assessing the eddy covariance technique for evaluating carbon dioxide exchange rates of ecosystems: past, present and future, Glob. Change Biol., 9, 479–492, 2003.

Baldocchi, D. D., Falge, E., Gu, L. H., Olson, R., Hollinger, D., Running, S., Anthoni, P., Bernhofer, C., Davis, K., Evans, R., Fuentes, J., Goldstein, A., Katul, G., Law, B., Lee, X. H., Malhi, Y., Meyers, T., Munger, W., Oechel, W., U, K. T. P., Pilegaard, K., Schmid, H. P., Valentini, R., Verma, S., Vesala, T., Wilson, K., and Wofsy, S.: FLUXNET: a new tool to study the temporal and spatial variability of ecosystem-scale carbon dioxide, water vapor, and energy flux densities, B. Am. Meteorol. Soc., 82, 2415–2434, 2001.

Bigger, C. M. and Oechel, W. C.: Nutrient effect on maximum photosynthesis in Arctic plants, Holarctic Ecol., 5, 158–163, 1982.

Björkman, O., Boardman, N. K., Anderson, J. M., Thorne, S. W., Goodchild, D. J., and Pyliotis, N. A.: Effect of light intensity during growth of Atriplex patula on the capacity of photosynthetic reactions, chloroplast components and structure, Carnegie I. Wash., 115–135, 1972.

BGD
11, 6419–6460, 2014

Burba, G. G., McDermitt, D. K., Grelle, A., Anderson, D. J., and Xu, L. K.: Addressing the influence of instrument surface heat exchange on the measurements of CO_2 flux from open-path gas analyzers, Glob. Change Biol., 14, 1854–1876, 2008.

Centritto, M., Brilli, F., Fodale, R., and Loreto, F.: Different sensitivity of isoprene emission, respiration and photosynthesis to high growth temperature coupled with drought stress in black poplar (Populus nigra) saplings, Tree Physiol., 31, 275–286, 2011.

Chapin, F. S. and Shaver, G. R.: Physiological and growth responses of arctic plants to a field experiment simulating climatic change, Ecology, 77, 822–840, 1996.

Chapin, F. S., Eugster, W., McFadden, J. P., Lynch, A. H., and Walker, D. A.: Summer differences among Arctic ecosystems in regional climate forcing, J. Climate, 13, 2002–2010, 2000.

Christensen, T. R., Jackowicz-Korczynski, M., Aurela, M., Crill, P., Heliasz, M., Mastepanov, M., and Friborg, T.: Monitoring the multi-year carbon balance of a subarctic palsa mire with micrometeorological techniques, Ambio, 41, 207–217, 2012.

Eugster, W., McFadden, J. P., and Chapin, F. S.: Differences in surface roughness, energy, and CO_2 fluxes in two moist tundra vegetation types, Kuparuk watershed, Alaska, USA, Arct. Antarct. Alp. Res., 37, 61–67, 2005.

Fahnestock, J. T., Jones, M. H., and Welker, J. M.: Wintertime CO_2 efflux from arctic soils: implications for annual carbon budgets, Global Biogeochem. Cy., 13, 775–779, 1999.

Falge, E., Baldocchi, D., Olson, R., Anthoni, P., Aubinet, M., Bernhofer, C., Burba, G., Ceulemans, R., Clement, R., Dolman, H., Granier, A., Gross, P., Grunwald, T., Hollinger, D., Jensen, N. O., Katul, G., Keronen, P., Kowalski, A., Lai, C. T., Law, B. E., Meyers, T., Moncrieff, H., Moors, E., Munger, J. W., Pilegaard, K., Rannik, U., Rebmann, C., Suyker, A., Tenhunen, J., Tu, K., Verma, S., Vesala, T., Wilson, K., and Wofsy, S.: Gap filling strategies for defensible annual sums of net ecosystem exchange, Agr. Forest Meteorol., 107, 43–69, 2001.

Frolking, S. E., Bubier, J. L., Moore, T. R., Ball, T., Bellisario, L. M., Bhardwaj, A., Carroll, P., Crill, P. M., Lafleur, P. M., McCaughey, J. H., Roulet, N. T., Suyker, A. E., Verma, S. B., Waddington, J. M., and Whiting, G. J.: Relationship between ecosystem productivity and photosynthetically active radiation for northern peatlands, Global Biogeochem. Cy., 12, 115–126, 1998.

Gilmanov, T. G., Verma, S. B., Sims, P. L., Meyers, T. P., Bradford, J. A., Burba, G. G., and Suyker, A. E.: Gross primary production and light response parameters of four Southern

BGD
11, 6419–6460, 2014

Plains ecosystems estimated using long-term CO_2-flux tower measurements, Global Biogeochem. Cy., 17, 1071, doi:10.1029/2002GB002023, 2003.
Givnish, T. J.: Adaptation to sun and shade – a whole-plant perspective, Aust. J. Plant Physiol., 15, 63–92, 1988.
Givnish, T. J., Montgomery, R. A., and Goldstein, G.: Adaptive radiation of photosynthetic physiology in the Hawaiian lobeliads: light regimes, static light responses, and whole-plant compensation points, Am. J. Bot., 91, 228–246, 2004.
Griffis, T. J., Rouse, W. R., and Waddington, J. M.: Interannual variability of net ecosystem CO_2 exchange at a subarctic fen, Global Biogeochem. Cy., 14, 1109–1121, 2000.
Groendahl, L., Friborg, T., and Soegaard, H.: Temperature and snow-melt controls on interannual variability in carbon exchange in the high Arctic, Theor. Appl. Climatol., 88, 111–125, 2007.
Hugelius, G., Bockheim, J. G., Camill, P., Elberling, B., Grosse, G., Harden, J. W., Johnson, K., Jorgenson, T., Koven, C. D., Kuhry, P., Michaelson, G., Mishra, U., Palmtag, J., Ping, C.-L., O'Donnell, J., Schirrmeister, L., Schuur, E. A. G., Sheng, Y., Smith, L. C., Strauss, J., and Yu, Z.: A new data set for estimating organic carbon storage to 3 m depth in soils of the northern circumpolar permafrost region, Earth Syst. Sci. Data, 5, 393–402, doi:10.5194/essd-5-393-2013, 2013.
Humphreys, E. R., Lafleur, P. M., Flanagan, L. B., Hedstrom, N., Syed, K. H., Glenn, A. J., and Granger, R.: Summer carbon dioxide and water vapor fluxes across a range of northern peatlands, J. Geophys. Res.-Biogeo., 111, G04011, doi:10.1029/2005JG000111, 2006.
IPCC: Summary for policymakers, in: Climate Change 2013: The Physical Science Basis. Contribution of Working Group I to the Fifth Assessment Report of the Intergovernmental Panel on Climate Change, edited by: Stocker, T. F., Qin, D., Plattner, G.-K., Tignor, M., Allen, S. K., Boschung, J., Nauels, A., Xia, Y., Bex, V., and Midgley, P. M., Cambridge, 1–29, 2013.
Jacovides, C. P., Tymvios, F. S., Asimakopoulos, D. N., Theofilou, K. M., and Pashiardes, S.: Global photosynthetically active radiation and its relationship with global solar radiation in the Eastern Mediterranean basin, Theor. Appl. Climatol., 74, 227–233, 2003.
Jones, M. H., Fahnestock, J. T., and Welker, J. M.: Early and late winter CO_2 efflux from arctic tundra in the Kuparuk River watershed, Alaska, USA, Arct. Antarct. Alp. Res., 31, 187–190, 1999.

BGD
11, 6419–6460, 2014

Kuhry, P., Ping, C. L., Schuur, E. A. G., Tarnocai, C., and Zimov, S.: Report from the International Permafrost Association: carbon pools in permafrost regions, Permafrost Periglac., 20, 229–234, 2009.
Kutzbach, L., Wille, C., and Pfeiffer, E.-M.: The exchange of carbon dioxide between wet arctic tundra and the atmosphere at the Lena River Delta, Northern Siberia, Biogeosciences, 4, 869–890, doi:10.5194/bg-4-869-2007, 2007.
Kwon, H. J., Oechel, W. C., Zulueta, R. C., and Hastings, S. J.: Effects of climate variability on carbon sequestration among adjacent wet sedge tundra and moist tussock tundra ecosystems, J. Geophys. Res.-Biogeo., 111, G03014, doi:10.1029/2005JG000036, 2006.
Lafleur, P. M. and Humphreys, E. R.: Spring warming and carbon dioxide exchange over low Arctic tundra in central Canada, Glob. Change Biol., 14, 740–756, 2008.
Lafleur, P. M., Humphreys, E. R., St Louis, V. L., Myklebust, M. C., Papakyriakou, T., Poissant, L., Barker, J. D., Pilote, M., and Swystun, K. A.: Variation in peak growing season net ecosystem production across the Canadian Arctic, Environ. Sci. Technol., 46, 7971–7977, 2012.
Laurila, T., Soegaard, H., Lloyd, C. R., Aurela, M., Tuovinen, J. P., and Nordstroem, C.: Seasonal variations of net CO_2 exchange in European Arctic ecosystems, Theor. Appl. Climatol., 70, 183–201, 2001.
Lindroth, A., Lund, M., Nilsson, M., Aurela, M., Christensen, T. R., Laurila, T., Rinne, J., Riutta, T., Sagerfors, J., Strom, L., Tuovinen, J. P., and Vesala, T.: Environmental controls on the CO_2 exchange in north European mires, Tellus B, 59, 812–825, 2007.
Loranty, M. M., Goetz, S. J., Rastetter, E. B., Rocha, A. V., Shaver, G. R., Humphreys, E. R., and Lafleur, P. M.: Scaling an instantaneous model of Tundra NEE to the Arctic landscape, Ecosystems, 14, 76–93, 2011.
Lund, M., Lafleur, P. M., Roulet, N. T., Lindroth, A., Christensen, T. R., Aurela, M., Chojnicki, B. H., Flanagan, L. B., Humphreys, E. R., Laurila, T., Oechel, W. C., Olejnik, J., Rinne, J., Schubert, P., and Nilsson, M. B.: Variability in exchange of CO_2 across 12 northern peatland and tundra sites, Glob. Change Biol., 16, 2436–2448, 2010.
Lund, M., Falk, J. M., Friborg, T., Mbufong, H. N., Sigsgaard, C., Soegaard, H., and Tamstorf, M. P.: Trends in CO_2 exchange in a high Arctic tundra heath, 2000–2010, J. Geophys. Res.-Biogeo., 117, G02001, doi:10.1029/2011JG001901, 2012.

BGD
11, 6419–6460, 2014

Marushchak, M. E., Pitkamaki, A., Koponen, H., Biasi, C., Seppala, M., and Martikainen, P. J.: Hot spots for nitrous oxide emissions found in different types of permafrost peatlands, Glob. Change Biol., 17, 2601–2614, 2011.

Marushchak, M. E., Kiepe, I., Biasi, C., Elsakov, V., Friborg, T., Johansson, T., Soegaard, H., Virtanen, T., and Martikainen, P. J.: Carbon dioxide balance of subarctic tundra from plot to regional scales, Biogeosciences, 10, 437–452, doi:10.5194/bg-10-437-2013, 2013.

McGuire, A. D., Anderson, L. G., Christensen, T. R., Dallimore, S., Guo, L. D., Hayes, D. J., Heimann, M., Lorenson, T. D., Macdonald, R. W., and Roulet, N.: Sensitivity of the carbon cycle in the Arctic to climate change, Ecol. Monogr., 79, 523–555, 2009.

McGuire, A. D., Christensen, T. R., Hayes, D., Heroult, A., Euskirchen, E., Kimball, J. S., Koven, C., Lafleur, P., Miller, P. A., Oechel, W., Peylin, P., Williams, M., and Yi, Y.: An assessment of the carbon balance of Arctic tundra: comparisons among observations, process models, and atmospheric inversions, Biogeosciences, 9, 3185–3204, doi:10.5194/bg-9-3185-2012, 2012.

Mooney, H. A., Bjorkman, O., and Collatz, G. J.: Photosynthetic acclimation to temperature in desert shrub, larrea-divaricata, 1. Carbon-dioxide exchange characteristics of intact leaves, Plant Physiol., 61, 406–410, 1978.

New, M., Lister, D., Hulme, M., and Makin, I.: A high-resolution data set of surface climate over global land areas, Clim. Res., 21, 1–25, 2002.

Niu, S. L., Li, Z. X., Xia, J. Y., Han, Y., Wu, M. Y., and Wan, S.: Climatic warming changes plant photosynthesis and its temperature dependence in a temperate steppe of northern China, Environ. Exp. Bot., 63, 91–101, 2008.

Niu, S. L., Luo, Y. Q., Fei, S. F., Yuan, W. P., Schimel, D., Law, B. E., Ammann, C., Arain, M. A., Arneth, A., Aubinet, M., Barr, A., Beringer, J., Bernhofer, C., Black, T. A., Buchmann, N., Cescatti, A., Chen, J. Q., Davis, K. J., Dellwik, E., Desai, A. R., Etzold, S., Francois, L., Gianelle, D., Gielen, B., Goldstein, A., Groenendijk, M., Gu, L. H., Hanan, N., Helfter, C., Hirano, T., Hollinger, D. Y., Jones, M. B., Kiely, G., Kolb, T. E., Kutsch, W. L., Lafleur, P., Lawrence, D. M., Li, L. H., Lindroth, A., Litvak, M., Loustau, D., Lund, M., Marek, M., Martin, T. A., Matteucci, G., Migliavacca, M., Montagnani, L., Moors, E., Munger, J. W., Noormets, A., Oechel, W., Olejnik, J., Kyaw, T. P. U., Pilegaard, K., Rambal, S., Raschi, A., Scott, R. L., Seufert, G., Spano, D., Stoy, P., Sutton, M. A., Varlagin, A., Vesala, T., Weng, E. S., Wohlfahrt, G., Yang, B., Zhang, Z. D., and Zhou, X. H.: Thermal optimality of

BGD
11, 6419–6460, 2014

net ecosystem exchange of carbon dioxide and underlying mechanisms, New Phytol., 194, 775–783, 2012.
Oberbauer, S. F. and Oechel, W. C.: Maximum CO_2-assimilation rates of vascular plants on an Alaskan Arctic Tundra slope, Holarctic Ecol., 12, 312–316, 1989.
Oberbauer, S. F., Starr, G., and Pop, E. W.: Effects of extended growing season and soil warming on carbon dioxide and methane exchange of tussock tundra in Alaska, J. Geophys. Res.-Atmos., 103, 29075–29082, 1998.
Oechel, W. C., Vourlitis, G. L., Hastings, S. J., Zulueta, R. C., Hinzman, L., and Kane, D.: Acclimation of ecosystem CO_2 exchange in the Alaskan Arctic in response to decadal climate warming, Nature, 406, 978–981, 2000.
Ow, L. F., Griffin, K. L., Whitehead, D., Walcroft, A. S., and Turnbull, M. H.: Thermal acclimation of leaf respiration but not photosynthesis in Populus deltoides x nigra, New Phytol., 178, 123–134, 2008a.
Ow, L. F., Whitehead, D., Walcroft, A. S., and Turnbull, M. H.: Thermal acclimation of respiration but not photosynthesis in Pinus radiata, Funct. Plant Biol., 35, 448–461, 2008b.
Parmentier, F. J. W., van der Molen, M. K., van Huissteden, J., Karsanaev, S. A., Kononov, A. V., Suzdalov, D. A., Maximov, T. C., and Dolman, A. J.: Longer growing seasons do not increase net carbon uptake in the northeastern Siberian tundra, J. Geophys. Res.-Biogeo., 116, G04013, doi:10.1029/2011JG001653, 2011.
Robinson, C. H., Michelsen, A., Lee, J. A., Whitehead, S. J., Callaghan, T. V., Press, M. C., and Jonasson, S.: Elevated atmospheric CO_2 affects decomposition of Festuca vivipara (L) Sm litter and roots in experiments simulating environmental change in two contrasting arctic ecosystems, Glob. Change Biol., 3, 37–49, 1997.
Rocha, A. V. and Shaver, G. R.: Burn severity influences postfire CO_2 exchange in arctic tundra, Ecol. Appl., 21, 477–489, 2011.
Ross, J.: The Radiation Regime and Architecture of Plant Stands, Tasks for Vegetation Sciences, The Hague, Boston, London, 391 pp., 1981.
Ruimy, A., Jarvis, P. G., Baldocchi, D. D., and Saugier, B.: CO_2 fluxes over plant canopies and solar radiation: a review, Adv. Ecol. Res., 26, 1–68, 1995.
Runkle, B. R. K., Sachs, T., Wille, C., Pfeiffer, E.-M., and Kutzbach, L.: Bulk partitioning the growing season net ecosystem exchange of CO_2 in Siberian tundra reveals the seasonality of its carbon sequestration strength, Biogeosciences, 10, 1337–1349, doi:10.5194/bg-10-1337-2013, 2013.

BGD
11, 6419–6460, 2014

Schuur, E. A. G., Bockheim, J., Canadell, J. G., Euskirchen, E., Field, C. B., Goryachkin, S. V., Hagemann, S., Kuhry, P., Lafleur, P. M., Lee, H., Mazhitova, G., Nelson, F. E., Rinke, A., Romanovsky, V. E., Shiklomanov, N., Tarnocai, C., Venevsky, S., Vogel, J. G., and Zimov, S. A.: Vulnerability of permafrost carbon to climate change: implications for the global carbon cycle, Bioscience, 58, 701–714, 2008.

Shaver, G. R., Billings, W. D., Chapin, F. S., Giblin, A. E., Nadelhoffer, K. J., Oechel, W. C., and Rastetter, E. B.: Global change and the carbon balance of Arctic ecosystems, Bioscience, 42, 433–441, 1992.

Shaver, G. R., Street, L. E., Rastetter, E. B., Van Wijk, M. T., and Williams, M.: Functional convergence in regulation of net CO_2 flux in heterogeneous tundra landscapes in Alaska and Sweden, J. Ecol., 95, 802–817, 2007.

Shaver, G. R., Rastetter, E. B., Salmon, V., Street, L. E., van de Weg, M. J., Rocha, A., van Wijk, M. T., and Williams, M.: Pan-Arctic modelling of net ecosystem exchange of CO_2, Philos. T. R. Soc. B, 368, 20120485. doi:10.1098/rstb.2012.0485, 2013.

Shurpali, N. J., Verma, S. B., Kim, J., and Arkebauer, T. J.: Carbon-dioxide exchange in a peatland ecosystem, J. Geophys. Res.-Atmos., 100, 14319–14326, 1995.

Skre, O. and Oechel, W. C.: Moss functioning in different Taiga ecosystems in Interior Alaska, 1. Seasonal, phenotypic, and drought effects on photosynthesis and response patterns, Oecologia, 48, 50–59, 1981.

Sorensen, P. L., Jonasson, S., and Michelsen, A.: Nitrogen fixation, denitrification, and ecosystem nitrogen pools in relation to vegetation development in the subarctic, Arct. Antarct. Alp. Res., 38, 263–272, 2006.

Street, L. E., Shaver, G. R., Williams, M., Van and Wijk, M. T.: What is the relationship between changes in canopy leaf area and changes in photosynthetic CO_2 flux in arctic ecosystems?, J. Ecol., 95, 139–150, 2007.

Street, L. E., Stoy, P. C., Sommerkorn, M., Fletcher, B. J., Sloan, V. L., Hill, T. C., and Williams, M.: Seasonal bryophyte productivity in the sub-Arctic: a comparison with vascular plants, Funct. Ecol., 26, 365–378, 2012.

SWIPA: Snow, Water, Ice, Permafrost in the Arctic, available at: http://www.amap.no/swipa/, 2011.

van der Molen, M. K., van Huissteden, J., Parmentier, F. J. W., Petrescu, A. M. R., Dolman, A. J., Maximov, T. C., Kononov, A. V., Karsanaev, S. V., and Suzdalov, D. A.: The growing season

BGD
11, 6419–6460, 2014

greenhouse gas balance of a continental tundra site in the Indigirka lowlands, NE Siberia, Biogeosciences, 4, 985–1003, doi:10.5194/bg-4-985-2007, 2007.
Vourlitis, G. L. and Oechel, W. C.: Landscape-scale CO_2, H_2O vapour and energy flux of moist-wet coastal tundra ecosystems over two growing seasons, J. Ecol., 85, 575–590, 1997.
Vourlitis, G. L. and Oechel, W. C.: Eddy covariance measurements of CO_2 and energy fluxes of an Alaskan tussock tundra ecosystem, Ecology, 80, 686–701, 1999.
Walker, D. A., Jia, G. J., Epstein, H. E., Raynolds, M. K., Chapin, F. S., Copass, C., Hinzman, L. D., Knudson, J. A., Maier, H. A., Michaelson, G. J., Nelson, F., Ping, C. L., Romanovsky, V. E., and Shiklomanov, N.: Vegetation-soil-thaw-depth relationships along a Low-Arctic bioclimate gradient, Alaska: synthesis of information from the ATLAS studies, Permafrost Periglac., 14, 103–123, 2003.
Walker, D. A., Raynolds, M. K., Daniels, F. J. A., Einarsson, E., Elvebakk, A., Gould, W. A., Katenin, A. E., Kholod, S. S., Markon, C. J., Melnikov, E. S., Moskalenko, N. G., Talbot, S. S., Yurtsev, B. A., and Team, C.: The Circumpolar Arctic vegetation map, J. Veg. Sci., 16, 267–282, 2005.
Westergaard-Nielsen, A., Lund, M., Hansen, B. U., and Tamstorf, M. P.: Camera derived vegetation greenness index as proxy for gross primary production in a low Arctic wetland area, ISPRS J. Photogramm., 83, 89–99, 2013.
Williams, M., Street, L. E., van Wijk, M. T., and Shaver, G. R.: Identifying differences in carbon exchange among arctic ecosystem types, Ecosystems, 9, 288–304, 2006.
Yuan, W., Luo, Y., Liang, S., Yu, G., Niu, S., Stoy, P., Chen, J., Desai, A. R., Lindroth, A., Gough, C. M., Ceulemans, R., Arain, A., Bernhofer, C., Cook, B., Cook, D. R., Dragoni, D., Gielen, B., Janssens, I. A., Longdoz, B., Liu, H., Lund, M., Matteucci, G., Moors, E., Scott, R. L., Seufert, G., and Varner, R.: Thermal adaptation of net ecosystem exchange, Biogeosciences, 8, 1453–1463, doi:10.5194/bg-8-1453-2011, 2011.

BGD
11, 6419–6460, 2014

Table 1. Site descriptions and eddy covariance measurement characteristics.

Code	Site	Country	Latitude	Longitude	Arctic type	Tundra type	EC gas analyzer
RU-Seid-SA	Seida	Russia	67°48′ N	64°01′ E	Subarctic	Mixed tundra	LI-7500
FI-Kaam-SA	Kaamanen	Finland	69°08′ N	27°17′ E	Subarctic	Fen	LI-6262
SE-Stord-SA	Stordalen	Sweden	68°20′ N	87°19′ E	Subarctic	Fen	LI-7500
NO-Ando-SA	Andøya	Norway	69°06′ N	15°155′ E	Subarctic	Bog	LI-7500
US-Anak-LA	Anaktuvuk	USA	68°56′ N	150°16′ W	Low Arctic	Mixed tundra	LI-7500
CA-Dar-LA	Daring Lake	Canada	64°52′ N	111°34′ W	Low Arctic	Mixed tundra	LI-7500
US-Ivot-LA	Ivotuk	USA	68°30′ N	155°21′ W	Low Arctic	Mixed tundra	ATDD, LI-7500
RU-Kyt-LA	Kytalyk	Russia	70°49′ N	147°29′ E	Low Arctic	Mixed tundra	LI-7500
GL-Nuuk-LA	Nuuk	Greenland	64°09′ N	51°20′ W	Low Arctic	Fen	LI-7000
RU-Sam-LA	Samoylov Island	Russia	72°22′ N	126°30′ E	Low Arctic	Mixed tundra	LI-7000
US-Barr-LA	Barrow	USA	71°19′ N	156°36′ W	Low Arctic	Wet sedge tundra	ATDD, LI-7500
GL-Zack-HA	Zackenberg	Greenland	74°28′ N	20°33′ W	High Arctic	Heath tundra	LI-6262, LI-7000

BGD
11, 6419–6460, 2014

Table 1. Continued.

Code	Sonic	Tower height	Years	Vegetation composition	Reference
RU-Seid-SA	Gill R3	3.95	2008	Sedge (*Eriophorum vaginatum*), vascular plants (*Rubus Chamaemorus, Vaccinium uliginosum, Ledums decumbens*); Moss (*Sphagnum spp., Dicranum spp., Drepanocladus aduncus, Pleurozium schreberi*); lichens (*Cladonia spp.*) and shrubs (*Betula nana* and *Salix spp., Vaccinium spp.*)	Marushchak et al. (2011)
FI-Kaam-SA	SWS-211	5	1997–2002	Sedges (*Eriophorium spp.*), dwarf shrubs (*Betula nana, Empetrum nigrum* and *Rubus chaemaemorus*), lichens (*Cladonia spp.* and *Cladonia spp.*) and mosses (*Spagnum* and *Dicranum spp.*)	Aurela et al. (2001)
SE-Stord-SA	Gill R3	3	2001–2008	Sedges (*Eriophorium vaginatum*), lichens (*Cladonia spp.*), mosses (*Sphagnum spp.*) and shrubs (*Empetrum nigrum*)	Christensen et al. (2012)
NO-Ando-SA	CSAT-3	3	2008–2011	Shrubs (*Empetrum nigrum*); sedges (*Eriophorum spp.* and *Carex spp.*); bryophytes (*Sphagnum spp.*); and lichens (*Cladonia spp.*)	Lund et al. (2014)
US-Anak-LA	CSAT-3	2.6	2008–2012	Tussock forming sedge (*Eriophorum spp.*); moss (*Sphagnum spp., Hylocomium spp.*); moss (*Sphagnum spp.*) and shrubs (*Betula nana, Salix pulchra*) and shrubs (*Betula nana, Vaccinium vitis-idaea, Ledum palustre* and *Rubus chamaemorus*)	Rocha and Shaver (2011)
CA-Dar-LA	Gill R3	4	2004–2007	Shrubs (*Empetrum nigrum, Ledum decumbens, Vaccinium vitis-idaea, Betula glandulosa, Vaccinium uliginosum* and *Rubus chamaemorus*); sedges (*Carex spp.*) and moss	Lafleur and Humphreys (2008)
US-Ivot-LA	Gill R3	3.8	2004, 2006	Tussock forming sedge (*Eriophorium vagiunatum, Carex begelowii, Dryas interdrifolia*); moss (*Sphagnum spp.*) and shrubs (*Betula nana, Salix pulchra*) and lichens	Kwon et al. (2006)
RU-Kyt-LA	Gill R3	4.7	2003–2010	Sedges (*Carex aquatilis, Eriophorium angustifolium*, and *Eriophorum vaginatum*); moss (*Sphagnum spp.*) and shrubs (*Betula nana, Salix pulchra*), and *Potentilla palustris*	Parmentier et al. (2011)
GL-Nuuk-LA	Gill R3	2.2	2008–2010	Sedges (*Carex rariflora, Eriophorum angustifolium*, and *Scirpus caespitosus*)	Westergaard-Nielsen et al. (2013)
RU-Sam-LA	Gill R3	3.65	2003, 2006	Sedges (*Carex spp*); moss (*Meesia longiseta, Limprichtia revolvens, Aulacomnium turgidum Hylocomium splendens* and *Timmia austriaca*); shrubs (*Dryas octopetala* and *Salix glauca*) and forbs (*Astragalus frigidus*)	Kutzbach et al. (2007)
US-Barr-LA	Gill R3	5	1998–2000	Sedges (*Carex aquatilis, Eriophorium spp*); mosses (*Calliergon ruchardsonii* and *Cinclidium subrotundum*) and lichens (*Peltigera spp.*)	Kwon et al. (2006)
GL-Zack-HA	Gill R2, Gill R3	3	2000–2010	Shrubs (*Cassiope tetragona, Dryas integrifolia* and *Vaccinium uliginosum*)	Lund et al. (2012)

BGD
11, 6419–6460, 2014

Table 2. Linear regressions between variables (environmental and vegetation properties) and LRC parameters: goodness of fit (r^2), slope and level of significance ($p < 0.1$).

Variables	LRC parameter	Slope	r^2	p	N
Maximum Leaf Area Index (LAI) and Jul Air temperature	F_{csat}	−2.4 and −0.2	0.92	0.001	9
	R_d	–	–	–	9
	α	–	–	–	9
	P_{sat}	−3.3 and −0.4	0.90	0.003	9
	F_{c1000}	−2.3 and −0.3	0.93	0.001	9
	LCP	–	–	–	9
Maximum Leaf Area Index (LAI)	F_{csat}	−2.8	0.75	0.006	9
	R_d	1.1	0.52	0.042	9
	α	0.02	0.61	0.023	9
	P_{sat}	−3.9	0.70	0.009	9
	F_{c1000}	−2.7	0.73	0.007	9
	LCP	–	–	–	9
Normalized Difference Vegetation Index (NDVI)	F_{csat}	−28.3	0.67	0.001	12
	R_d	10.4	0.40	0.026	12
	α	0.1	0.25	0.09	12
	P_{sat}	−38.7	0.61	0.003	12
	F_{c1000}	−26.0	0.59	0.004	12
	LCP	–	–	–	12
Jul Air temperature	F_{csat}	−0.3	0.32	0.055	12
	R_d	0.1	0.26	0.094	12
	α	–	–	–	12
	P_{sat}	−0.4	0.32	0.056	12
	F_{c1000}	−0.3	0.35	0.043	12
	LCP	–	–	–	12
Peak season PPFD	F_{csat}	–	–	–	12
	R_d	–	–	–	12
	α	–	–	–	12
	P_{sat}	–	–	–	12
	F_{c1000}	–	–	–	12
	LCP	0.2	0.52	0.008	12

BGD
11, 6419–6460, 2014

Table 3. Light response curve parameters (F_{csat}, R_d, α, P_{sat}, F_{c1000}, LCP), fitting period and related statistics, and variables (environmental and vegetation properties) for the study sites. Note that assimilation parameters (F_{csat}, P_{sat}, F_{c1000}) are reported as negative values so as to demonstrate that they represent uptake from the atmosphere by the ecosystem.

Study sites	Peak period	F_{csat} ($\mu mol\,m^{-2}\,s^{-1}$)	R_d ($\mu mol\,m^{-2}\,s^{-1}$)	α	P_{sat} ($\mu mol\,m^{-2}\,s^{-1}$)
RU-Seid-SA	24 Jul–6 Aug	−8.0	3.9	0.057	−11.9
FI-Kaam-SA	24 Jul–6 aug (±10 days)	−4.7 ± 0.6	1.7 ± 0.2	0.020 ± 0.002	−6.4 ± 0.7
SE-Stord-SA	23 Jul–5 Aug (±16 days)	−6.2 ± 1.9	2.0 ± 0.5	0.025 ± 0.005	−8.2 ± 1.9
NO-Ando-SA	9 Jul–22 Jul (±18 days)	−4.0 ± 0.4	1.1 ± 0.1	0.018 ± 0.005	−5.2 ± 0.3
US-Anak-LA	12 Jul–25 Jul (±8 days)	−4.6 ± 0.3	1.2 ± 0.4	0.017 ± 0.005	−5.7 ± 0.3
CA-Dar-LA	9 Jul–22 Jul (±16 days)	−3.3 ± 0.5	1.0 ± 0.1	0.012 ± 0.002	−4.4 ± 0.5
US-Ivot-LA	23 Jul–5 Aug (±4 days)	−4.7 ± 0.9	1.2 ± 0.5	0.012 ± 0.011	−5.9 ± 0.4
RU-Kyt-LA	24 Jul–6 Aug (±10 days)	−5.4 ± 0.8	1.6 ± 0.6	0.020 ± 0.006	−7.0 ± 1.1
GL-Nuuk-LA	30 Jun–13 Jul (±17 days)	−4.0 ± 0.7	1.8 ± 0.5	0.019 ± 0.003	−5.8 ± 0.9
RU-Sam-LA	30 Jul–12 Aug (±13 days)	−1.7 ± 0.3	0.6 ± 0.3	0.013 ± 0.001	−2.3 ± 0.6
US-Barr-LA	25 Jul–7 Aug (±8 days)	−4.4 ± 1.4	1.2 ± 0.5	0.035 ± 0.031	−5.6 ± 1.9
GL-Zack-HA	17 Jul–30 Jul (±9 days)	−1.6 ± 0.2	1.0 ± 0.3	0.011 ± 0.003	−2.6 ± 0.4
Coefficient of variation (CV):		0.39	0.52	0.58	0.41

BGD
11, 6419–6460, 2014

Table 3. Continued.

Study sites	F_{c1000} ($\mu mol\,m^{-2}\,s^{-1}$)	LCP ($\mu mol\,m^{-2}\,s^{-1}$)	r^2	N	NDVI	LAI	Jul temperature (°C)
RU-Seid-SA	−7.9	80	0.69	253	0.74	1.85	15.8
FI-Kaam-SA	−4.4 ± 0.5	100 ± 15	0.91	561	0.69 ± 0.03	0.70	13.9 ± 0.4
SE-Stord-SA	−5.7 ± 1.6	97 ± 32	0.79	353	0.68 ± 0.02	> 2	11.8 ± 1.3
NO-Ando-SA	−3.9 ± 0.4	73 ± 18	0.77	373	0.70 ± 0.06	–	10.9 ± 0.7
US-Anak-LA	−4.2 ± 0.3	77 ± 10	0.51	296	0.68 ± 0.02	–	15.8 ± 1.0
CA-Dar-LA	−3.0 ± 0.3	102 ± 10	0.73	428	0.60 ± 0.01	0.70	12.4 ± 1.5
US-Ivot-LA	−3.1 ± 1.2	156 ± 87	0.73	582	0.71 ± 0.03	0.71	12.2 ± 2.9
RU-Kyt-LA	−4.9 ± 0.8	91 ± 20	0.78	463	0.68 ± 0.03	0.78	10.6 ± 3.2
GL-Nuuk-LA	−3.8 ± 0.5	111 ± 22	0.74	363	0.67 ± 0.01	–	10.1 ± 0.2
RU-Sam-LA	−1.7 ± 0.3	53 ± 26	0.59	246	0.62 ± 0.05	0.30	9.2 ± 0.1
US-Barr-LA	−3.6 ± 1.2	50 ± 25	0.42	569	0.63	1.5	4.7 ± 1.0
GL-Zack-HA	−1.5 ± 0.2	113 ± 19	0.67	407	0.56 ± 0.05	0.30	6.6 ± 1.2
Coefficient of variation (CV):	0.42	0.3	0.18	0.28	0.07	0.63	0.29

BGD
11, 6419–6460, 2014

Table A1. Light response curve (LRC) parameters for peak period in 2008.

Study sites	2008 Peak period	F_{csat} ($\mu mol\,m^{-2}\,s^{-1}$)	R_d ($\mu mol\,m^{-2}\,s^{-1}$)	α	P_{sat} ($\mu mol\,m^{-2}\,s^{-1}$)	F_{c1000} ($\mu mol\,m^{-2}\,s^{-1}$)	r^2	N	Jul 2008 temperature (°C)
US-Anak-LA	16 Jul–29 Jul	−4.4	1.4	0.018	−5.8	−4.2	0.50	243	11.7
NO-Ando-SA	31 Jun–13 Jul	−3.5	1.2	0.014	−4.7	−3.3	0.82	470	10.5
RU-Kyt-LA	7 Aug–20 Aug	−6.1	1.6	0.016	−7.7	−5.2	0.75	484	8.4
GL-Nuuk-LA	6 Jul–19 Jul	−3.8	1.2	0.016	−5.0	−3.6	0.67	346	10.1
RU-Seid-SA	24 Jul–6 Aug	−8.0	3.9	0.057	−11.9	−7.9	0.69	253	15.8
SE-Stord-SA	25 Jul–7 Aug	−8.0	1.4	0.022	−9.4	−7.2	0.67	358	11.3
GL-Zack-HA	23 Jul–5 Aug	−1.7	1.1	0.015	−2.8	−1.7	0.67	327	8.7
Mean ± SD		−5.1 ± 2.4	1.7 ± 1.0	0.023 ± 0.015	−6.8 ± 3.1	−4.7 ± 2.2	0.7 ± 0.1	354 ± 95	10.9 ± 2.5

BGD
11, 6419–6460, 2014

Table A2. List of symbols.

Name	Units	Description
α, α_2	–	Modeled quantum efficiency/light use efficiency/initial slope of light response curve. (Eqs. 1 and 2)
F_{c1000}	$\mu mol\,m^{-2}\,s^{-1}$	Modeled CO_2 flux when light (PPFD) is $1000\,\mu mol\,m^{-2}\,s^{-1}$ (Eq. 1)
F_{csat}	$\mu mol\,m^{-2}\,s^{-1}$	Modeled CO_2 flux at light saturation. This represents the point when further increases in light do not affect the NEE (Eq. 1)
GPP	$\mu mol\,m^{-2}\,s^{-1}$	Gross primary production/Photosynthesis. CO_2 uptake from the atmosphere by the vegetation.
P_{sat}	$\mu mol\,m^{-2}\,s^{-1}$	Potential photosynthesis at light saturation. Calculated as $F_{csat} + R_d$ (Eq. 1)
LCP	$\mu mol\,m^{-2}\,s^{-1}$	Light compensation point. PPFD level when ecosystem switches from net daily source to sink of CO_2 (Eq. 1)
NEE	$\mu mol\,m^{-2}\,s^{-1}$	Measured half hourly net ecosystem exchange rate
P_{max}	$\mu mol\,m^{-2}\,s^{-1}$	Modeled potential photosynthesis at light saturation (Eq. 2)
PPFD	$\mu mol\,m^{-2}\,s^{-1}$	Measured half hourly photosynthetic photon flux density
R	$\mu mol\,m^{-2}\,s^{-1}$	Modeled dark or basal respiration/intercept of the light response curve (Eq. 2)
R_d	$\mu mol\,m^{-2}\,s^{-1}$	Modeled dark or basal respiration/intercept of the light response curve (Eq. 1)

BGD
11, 6419–6460, 2014

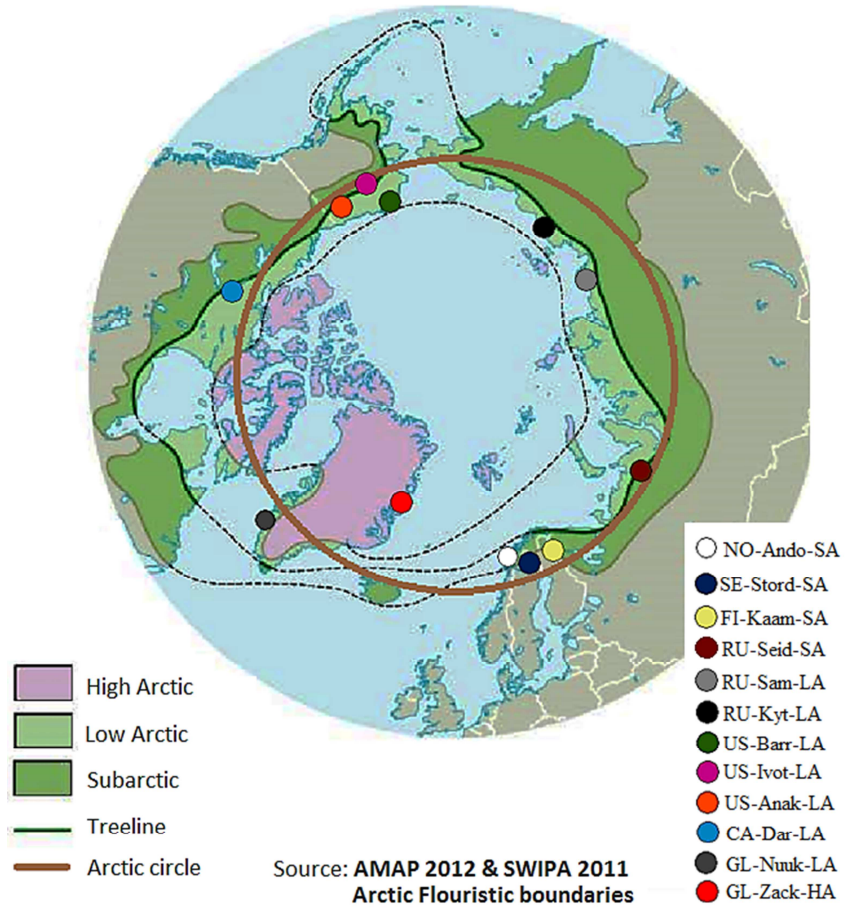

Fig. 1. Location of study sites in a circumpolar context. Map shows classification according Arctic floristic boundaries (AMAP, 1998).

BGD
11, 6419–6460, 2014

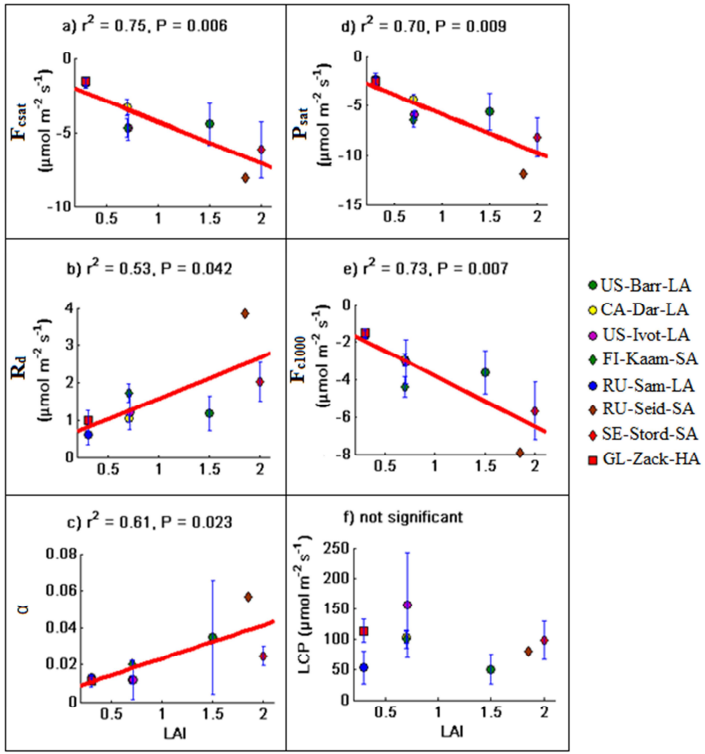

Fig. 2. Relationships between maximum leaf are index (LAI) and **(a)** light saturation NEE, F_{csat}; **(b)** dark respiration, R_d; **(c)** rate of carbon assimilation with initial increase in light, α; **(d)** potential photosynthesis at light saturation, P_{sat}; **(e)** NEE when PPFD is 1000 µmol m^{-2} s^{-1},F_{c1000} and **(f)** light compensation point (LCP). Red line represents linear fit between maximum LAI and LRC parameters while error bars are standard deviations.

BGD
11, 6419–6460, 2014

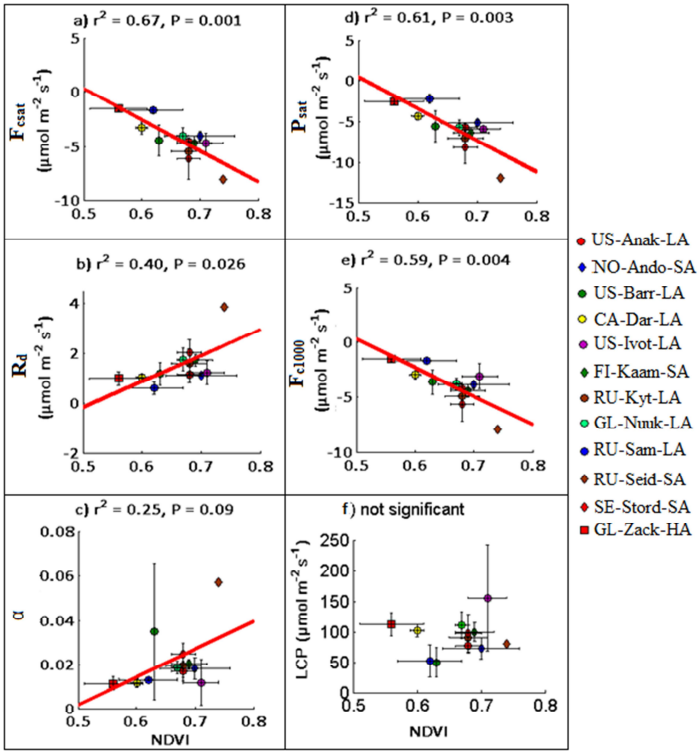

Fig. 3. Relationships between peak season NDVI and **(a)** light saturation NEE, F_{csat}; **(b)** dark respiration, R_d; **(c)** rate of carbon assimilation with initial increase in light, α; **(d)** potential photosynthesis at light saturation, P_{sat}; **(e)** NEE when PPFD is 1000 µmol m^{-2} s^{-1}, F_{c1000} and **(f)** light compensation point (LCP). Red line represents linear fit between peak season NDVI and LRC parameters while error bars are standard deviations.

BGD
11, 6419–6460, 2014

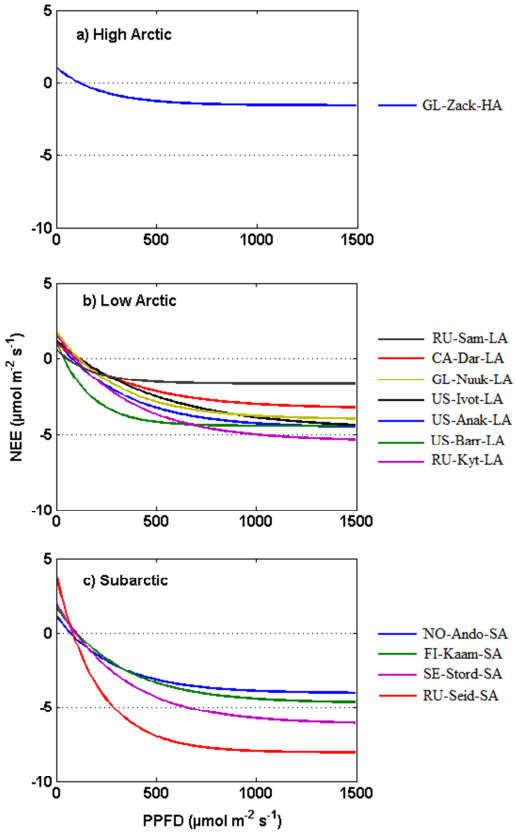

Fig. 4. Light response curves across the Arctic tundra, **(a)** High Arctic sites, **(b)** Low Arctic sites, **(c)** Subarctic sites. Classification was done according to Arctic floristic boundaries (AMAP, 1998)

BGD
11, 6419–6460, 2014

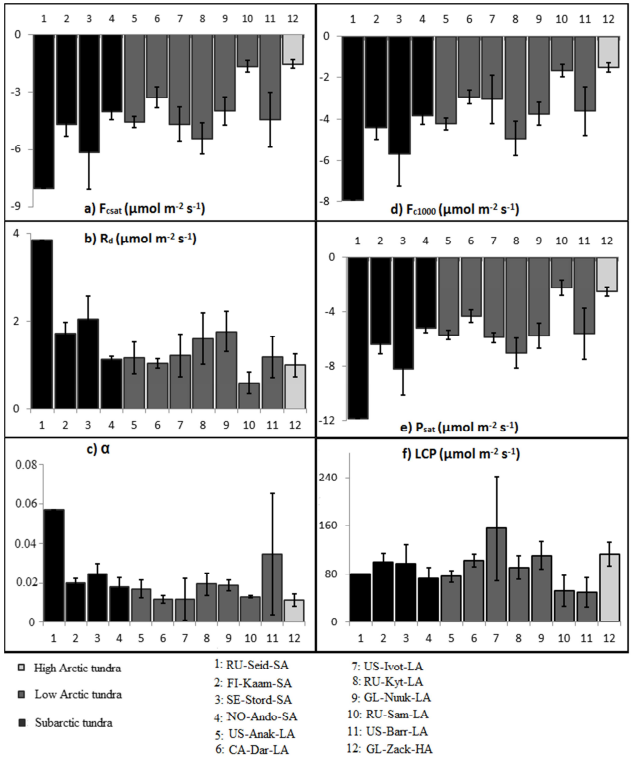

Fig. 5. Variability in LRC parameters among Arctic tundra sites. **(a)** flux at light saturation (F_{csat}); **(b)** dark respiration (R_d); **(c)** initial light use efficiency (α); **(d)** potential photosynthesis at light saturation (P_{sat}); **(e)** flux when PPFD = 1000 µmol m^{-2} s^{-1} (F_{c1000}); and **(f)** light compensation point (LCP). Illustrated according to mean July temperature in different tundra types.

BGD
11, 6419–6460, 2014

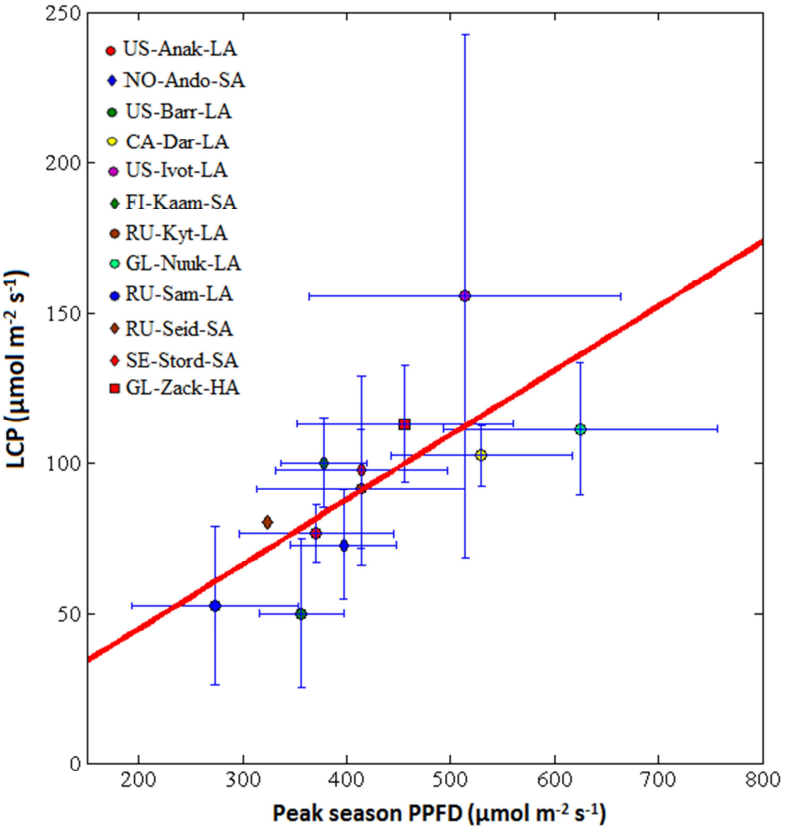

Fig. 6. Averaged peak season PPFD (light) control on light compensation point (LCP) parameter. $r^2 = 0.5$, $p = 0.008$. Ecosystems in regions prone to high light tend to be adapted to such conditions with a correspondingly high LCP.

BGD
11, 6419–6460, 2014

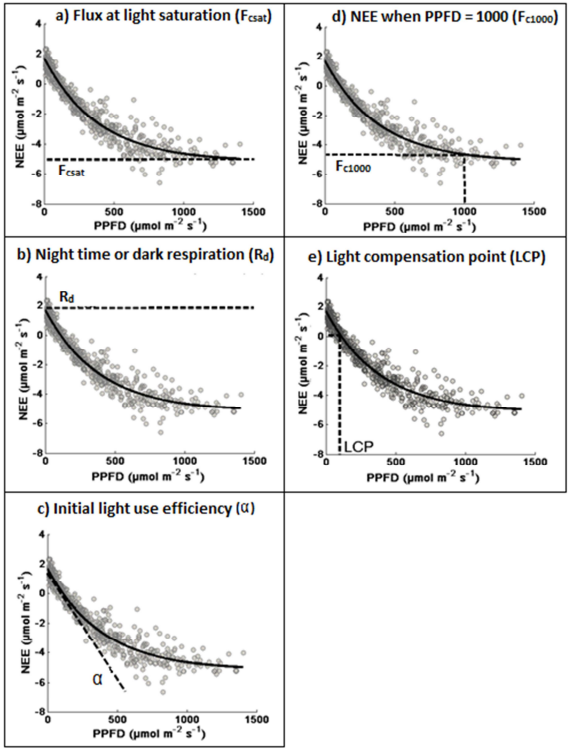

Fig. B1. Parameterization of LRC (Eq. 1). Continuous lines show the shape of the light response curves while broken lines illustrate parameters of the light response curves; **(a)** flux at light saturation; **(b)** dark respiration (when PPFD = 0 $\mu mol\,m^{-2}\,s^{-1}$); **(c)** initial light use efficiency; **(d)** NEE when PPFD = 1000 $\mu mol\,m^{-2}\,s^{-1}$ and **(e)** light compensation point PPFD when NEE = 0 $\mu mol\,m^{-2}\,s^{-1}$. Potential photosynthesis at light saturation (P_{sat}) was calculated as a theoretical parameter by adding F_{csat} and R_d.

BGD
11, 6419–6460, 2014

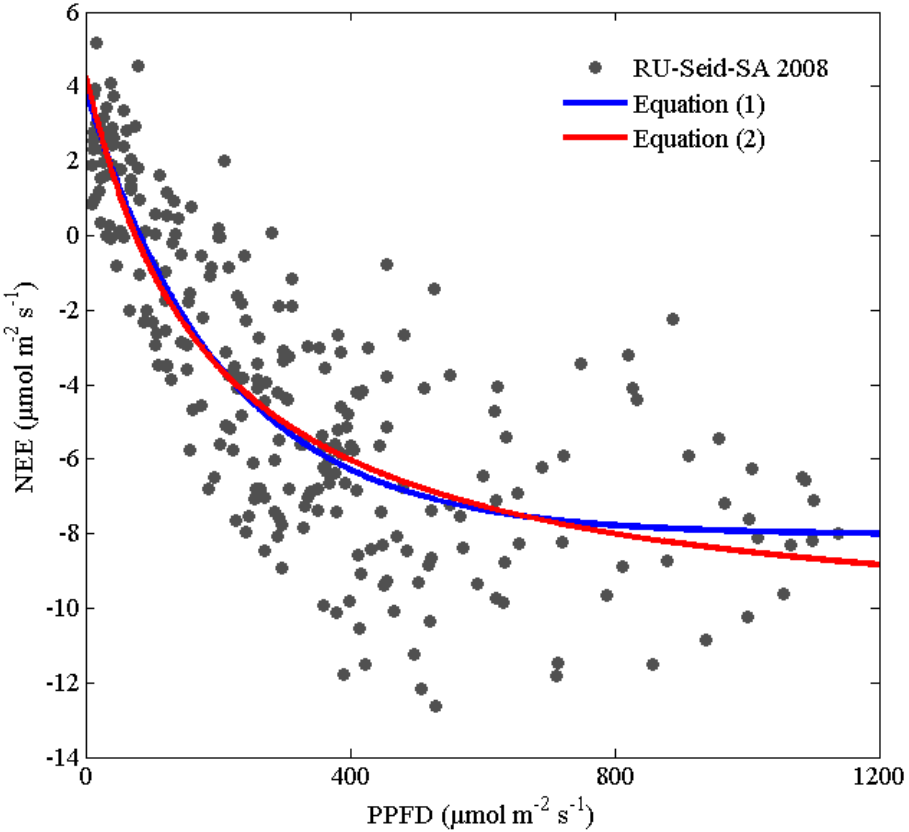

Fig. B2. Comparing Eqs. (1) and (2) using Seida 2008 peak season. The LRC curves suggest that the parameters R_d and α from Eq. (1) are comparable with R and α_2 from Eq. (2).

BGD
11, 6419–6460, 2014

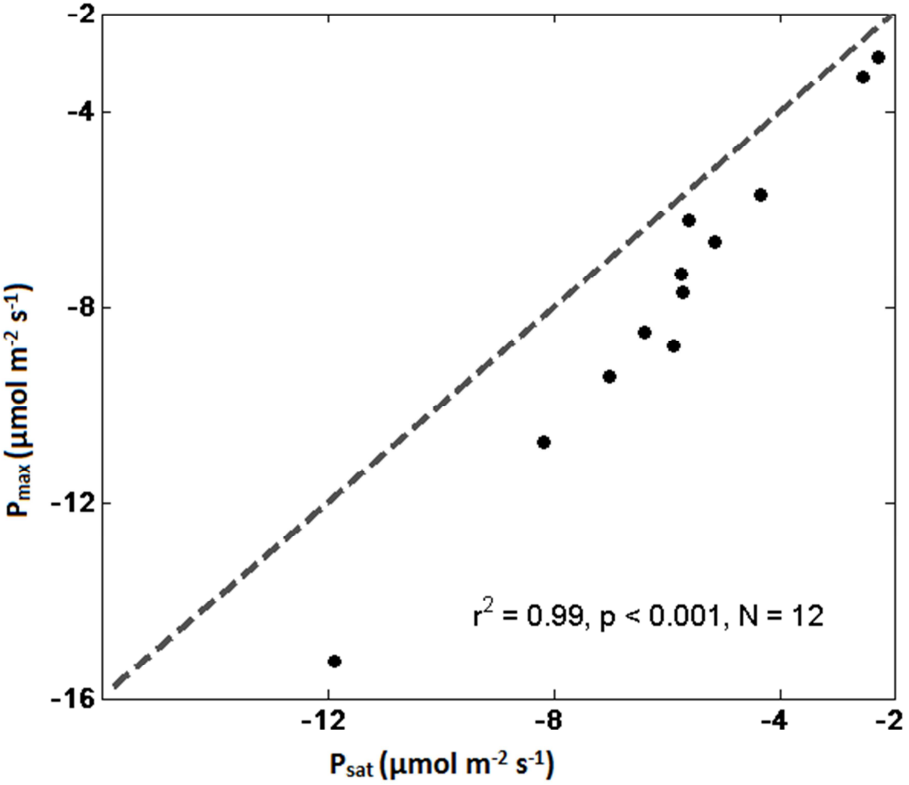

Fig. B3. Correlations between Eq. (1) (Falge et al., 2001) and (2) (Ruimy et al., 1995) using photosynthesis at light saturation. Potential photosynthesis at light saturation (P_{sat}) was calculated as the sum of F_{csat} and R_d in Eq. (1) (Falge et al., 2001; Lindroth et al., 2007) and was estimated by P_{max} in Eq. (2) (Frolking et al., 1998; Laurila et al., 2001; Ruimy et al., 1995) based on the 12 sites in this study. Broken line represents the 1 : 1 line.

BGD
11, 6419–6460, 2014

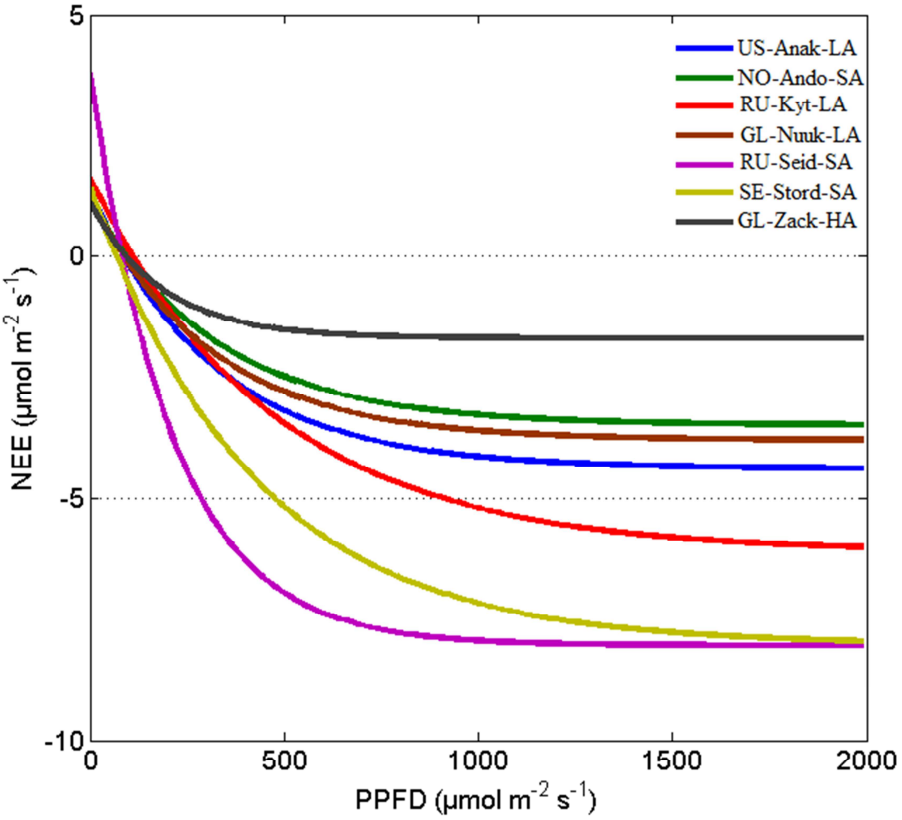

Fig. B4. Comparing LRC curves for peak period 2008 shows that F_{csat} for RU-Seid-SA may be comparable to SE-Stord-SA but differs in terms of α and R_d. Also, the LRC for RU-Seid-SA shows a stronger and unique curvature.

BGD
11, 6419–6460, 2014